

DOE/ER/45676

**Solid Solubilities of Pu, U, Gd and Hf in Candidate Ceramic
Nuclear Wasteforms**

Final Report – 09/12/1997 – 09/14/2000

**E. R. Vance
M. L. Carter
G. R. Lumpkin
R. A. Day
B. D. Begg**

April 2001

Work Performed Under Contract No. DE-FG07-96ER45676

**For
U.S. Department of Energy
Office of Energy Research
Washington, DC**

**By
Australian Nuclear Science and Technology Organization
Menai, NSW 2234, Australia**

DOE/ER/45676

**SOLID SOLUBILITIES OF Pu, U, Gd AND Hf IN CANDIDATE CERAMIC
NUCLEAR WASTEFORMS**

FINAL REPORT
09/12/1997 – 09/14/2000

E. R. Vance
M. L. Carter
G. R. Lumpkin
R. A. Day
B. D. Begg

April 2001

Work Performed Under Contract No. DE-FG07-96ER45676

Prepared for the
U.S. Department of Energy
Office of Energy Research
Washington, DC

Prepared by
Australian Nuclear Science and Technology Organization
Menai, NSW 2234, Australia

SOLID SOLUBILITIES OF Pu, U, Gd and Hf IN CANDIDATE CERAMIC NUCLEAR WASTEFORMS

E. R. VANCE, M. L. CARTER, G. R. LUMPKIN, R. A DAY and
B. D. BEGG, Materials Division, Australian Nuclear Science and
Technology Organisation, Menai, NSW 2234, Australia.

April 2001

FINAL REPORT (USDOE Grant No. DE-FG07-97ER45676)

EXECUTIVE SUMMARY

This work addresses the solid solubility of Pu, as well as U, Gd and Hf, in candidate ceramics for immobilisation of high-level nuclear waste. The experimental approach was to saturate each phase by adding more than the solid solubility limit of the given cation, using a nominated substitutional scheme, and then analysing the candidate phase that formed to evaluate the solid solubility limit under the firing conditions. Confirmation that the solid solution limit had been reached insofar as other phases rich in the cation of interest was also required.

The candidate phases were monazite, titanite, zirconolite, perovskite, apatite, pyrochlore, and brannerite. The valences of Pu and U were typically deduced from the firing atmosphere, and charge balancing in the candidate phase composition as evaluated from electron microscopy, although in some cases it was measured directly by X-ray absorption and diffuse reflectance (DRS) spectroscopies (for U).

Tetravalent Pu and U have restricted (< 0.1 formula units) solid solubilities in apatite, titanite and perovskite. Trivalent Pu has a larger solubility in apatite and perovskite than Pu^{4+} . U^{3+} appears to be a credible species in reduced perovskite with a solubility of ~ 0.25 f.u., as against ~ 0.05 f.u. for U^{4+} . Pu^{4+} is a viable species in monazite and is promoted at lower firing temperatures ($\sim 800^\circ\text{C}$) in an air atmosphere. Hf solubility is restricted in apatite, monazite (< 0.1 f.u.), but is ~ 0.2 and 0.5 f.u. respectively in brannerite and titanite respectively. Gd solubility is extended in all phases except for titanite (~ 0.3 f.u.). U^{5+} was identified by DRS observations of absorption

bands in the visible/near infrared photon energy ranges in brannerite and zirconolite, and U^{4+} in zirconolite was similarly identified.

SECTIONS

1. INTRODUCTION
2. Pu
3. U
4. Gd AND Hf
5. DISCUSSION AND CONCLUSIONS
4. REFERENCES
5. PRESENTATIONS AND PAPERS BASED ON THIS PROJECT

1. INTRODUCTION

The present work relates to the immobilisation of Pu. In the US, U will accompany Pu in many cases (indeed in the current plans for immobilisation of surplus Pu, twice as much U as Pu will be present in the titanate ceramic selected by the US Department of Energy). Gd and Hf are typically incorporated in Pu-bearing wasteforms as neutron absorbers. Therefore the scope of the present work, while primarily directed at the solid solubility of Pu in candidate ceramic phases, also addresses the solubility of U as well as the neutron absorbers, Hf and Gd. Many data pertaining to the chosen ceramic phases were known before the work commenced, but a detailed survey had not been done, especially when the different possible valences of U and Pu were considered. To define the solid solubility limit of a given species, we saturated the phase with an excess of the species, according to a nominated charge compensation scheme, and measured by scanning electron microscopy the concentration of guest ions in the phase of interest, as well as confirming that the solubility limit had been exceeded. In each of the following sections, we will review known data in each phase and then present our new findings, referring where appropriate to our own papers which are appended to this report.

The candidate ceramics and some of their properties are indicated in Table 1.

Table 1. Candidate ceramics considered in the present work.

Phase	Structure	Melting Point (°C)	Density (g/cm ³).
Monazite (CePO ₄)	Monoclinic	~ 2200	5.2
Apatite (Ca ₂ Nd ₈ (SiO ₄) ₆ O ₂)	Hexagonal	> 1650	5.5
Zirconolite (CaZrTi ₂ O ₇)	Monoclinic	~ 1600	4.5
Pyrochlore (CaPuTi ₂ O ₇)	Cubic	~ 1500	6.0
Titanite (CaTiSiO ₅)	Monoclinic	1380	3.5
Perovskite (CaTiO ₃)	Orthorhombic	~ 1900	4.0
Brannerite (UTi ₂ O ₆)	Monoclinic	~ 1500	6.4

Note that all these phases can include many different ions. Incorporation is generally controlled by similarities in ionic size and charge states of the ion and the host lattice site, once charge compensation mechanisms have been taken into account. In monazite, trivalent rare earths and trivalent/tetravalent actinides can be substituted on the Ce site. Such rare earths and actinides will substitute on the Ca and rare earth sites in apatite, the Ca and Zr sites in zirconolite, the (Ca/Pu) site of pyrochlore, the Ca site in titanite and perovskite, and the U site in brannerite. The valences adopted by the variable-valence ions depend on the oxygen fugacity of the firing atmosphere, and the crystal-chemical stabilisation energy in the particular site in which the ions are incorporated.

Materials in the present work were made by the alkoxide/nitrate route[1], using Ti and Zr as the metal propoxide and butoxide respectively mixed in ethanol, and

hydrolysed by an aqueous solution of metal nitrates. After stir-drying and calcination in air, argon or 3% H_2/N_2 at 750°C for 1 h, the calcines were wet-milled, dried, pelletised and then sintered in air, argon, or the H_2/N_2 . When sintering was carried out in argon the oxygen partial pressure was monitored by a zirconia probe (Type DL, Australian Oxytrol Systems Pty. Ltd., Eaglehawk, Victoria 3556, Australia) and was $\sim 10^{-5}$ atm.

Scanning electron microscopy (SEM) was carried out with a JEOL 6400 instrument operated at 15 keV, and fitted with a Tracor Northern Voyager IV X-ray microanalysis System (EDS). A comprehensive set of standards was used for quantitative work, giving a high degree of accuracy [2]. Powder X-ray diffraction analyses were conducted with a Siemens D500 diffractometer using $\text{Co K}\alpha$ radiation.

Transmission electron microscopy (TEM) was carried out using a JEOL 2000fxII machine fitted with a wide-bore pole piece and operated at 200 kV. The instrument was calibrated for selected area diffraction work for a range of objective lens currents using a gold standard. Phase compositions were determined using a Link ISIS solid state X-ray detector and analyser. This system has been calibrated using a wide range of natural and synthetic reference materials. Detailed analytical procedures for zirconolite and an assessment of precision and accuracy are given elsewhere [3]. Although peak fitting errors are typically below 0.7% relative for a synthetic zirconolite test sample, precision for the mean of a group of analyses is typically 1-3% relative.

To study U valences, XANES was performed on Line 4-2 at Stanford Synchrotron Research Laboratory. UTi_2O_6 (brannerite) and CaUO_4 were used as U^{4+} and U^{6+} valence standards respectively. Diffuse reflectance spectroscopy was carried out on

fine powders using a Cary 5 instrument, with the raw data being transformed to Kubelka-Munk absorption vs. wavelength plots.

2. PLUTONIUM

Before discussing our work on finding Pu solubilities in the phases of interest, we will indicate relevant previous work. Dilute amounts of trivalent Pu in monazite had been studied by electron spin resonance techniques [4], and the end-member PuPO_4 (Pu^{3+}) is well known and can be formed in an air atmosphere [5]. The progressive replacement of Zr in zirconolite by Pu^{4+} is known to cause a transition to pyrochlore ($\text{CaPuTi}_2\text{O}_7$) at ~ 0.7 f.u. of Pu [6], and the behaviour of 0.1 f.u. of Pu^{4+} substituting for Zr in zirconolite was reported earlier [7]. Perovskite structures containing Pu^{3+} (e.g. PuAlO_3) can be formed in argon or hydrogen firing atmospheres and Pu^{4+} -bearing perovskites (e.g. BaPuO_3) can be formed in air [8]. However the solubility of Pu^{4+} in CaTiO_3 was not known. The (tetravalent) Pu version of brannerite, PuTi_2O_6 , does not readily form as a single phase, but $\sim 75\%$ yields of the endmember were reported in preparations fired at 1525°C , just below the melting point of the preparation [9]. The pyrochlore, $\text{CaPuTi}_2\text{O}_7$, has been reported at $\sim 98\%$ yields on firing in air at 1500°C , again just below the melting point of the preparation [8]; broadly similar results had already been reported by Clinard et al.[10].

Present work is now described. An attempt was made to substitute Pu^{4+} in monazite via equimolar substitution of Ca and Pu for Ce. Thus it was expected that $\text{Ca}_{0.5}\text{Pu}_{0.5}\text{PO}_4$ stoichiometry (tetravalent Pu) would yield single-phase monazite, by comparison with the result for U analogues[11]. However microanalysis indicated that while this occurred in samples heated in air at 800°C , a higher firing temperature of 1400°C yielded a Pu/Ca ratio that was > 1 . This suggests that only 40% of the Pu was in

the +4 state, with the rest being trivalent. The reason for this behaviour is not known, but it presumably illustrates that the rare earth site strongly prefers trivalent occupancy.

A sample of $\text{Ca}_{0.7}\text{Pu}_{0.3}\text{Ti}_{0.7}\text{Al}_{0.3}\text{O}_3$ stoichiometry and designed to form perovskite was fired at 1400°C in argon for 24 h and the sample was indeed found to be essentially single-phase perovskite. This was consistent with Pu being trivalent, which was not surprising since perovskite-structured PuAlO_3 (Pu^{3+}) is a known compound on firing in a neutral/reducing atmosphere (see above). Another sample of $\text{Ca}_{0.7}\text{Pu}_{0.3}\text{Ti}_{0.4}\text{Al}_{0.6}\text{O}_3$ stoichiometry (targeted as perovskite with Pu as Pu^{4+}) was fired for 24 h at 1400°C in air, and the solid solubility limit of Pu^{4+} was found to be 0.13 f.u., with excess PuO_2 being observed.

A sample of $\text{Ca}_{0.9}\text{Pu}_{0.1}\text{Ti}_{0.8}\text{Al}_{0.2}\text{SiO}_5$ nominal stoichiometry, targeted as titanite, and fired in air at 1250°C was found to incorporate only 0.02 f.u. of Pu, presumably as Pu^{4+} , while another titanite sample of $\text{Ca}_{0.7}\text{Pu}_{0.3}\text{Ti}_{0.7}\text{Al}_{0.3}\text{SiO}_5$ (Pu targeted as Pu^{3+}) melted on firing in Ar at 1250°C. On firing a calcined precursor at 1200°C, 0.05 f.u. of Pu was incorporated in the titanite, with the increase of Pu incorporation indicating that some of the Pu was trivalent. The undissolved Pu formed PuO_2 in both cases.

Difficulties of forming phosphate apatites having grain sizes large enough to do accurate microanalysis led to the study of Pu incorporation in silicate apatites. Firing material of $\text{Ca}_2\text{Gd}_7\text{Pu}(\text{SiO}_4)_6\text{O}_2$ apatite stoichiometry for 20 h in argon or air revealed that Pu solubilities were 0.6 f.u., with PuO_2 appearing as an extra phase. Firing in H_2/N_2 at 1350°C led to incorporation of all the Pu in the apatite so it is deduced that the Pu is present as Pu^{3+} . In this case, and that the Pu incorporated in the apatites fired in air and argon was tetravalent. The higher solubility (> 1 f.u.) under reducing conditions is

consistent with the extensive solubility (8 f.u.) of light rare earths and the similarities of the ionic sizes of Pu^{3+} and the trivalent light rare earths. A further preparation of $\text{Ca}_2\text{Pu}_8(\text{SiO}_4)\text{O}_2$ stoichiometry was prepared in H_2/N_2 at 1350°C to find the limit of Pu^{3+} incorporation and the sample was very close to single-phase .

3. URANIUM

The incorporation of U in pyrochlore, zirconolite, brannerite, and monazite was known to be extensive[11,12] but only small amounts of U had been incorporated in perovskite, apatite and titanite. Hence we studied these latter phases.

For perovskite, firing in argon at 1400°C allows U^{4+} to enter the Ca site if two Al ions per U ion are present in the Ti site, and the solubility limit of U^{4+} was found as ~ 0.05 f.u. However in perovskite-structured samples of $Ca_{(1-x)}U_xTi_{(1-x)}Al_xO_3$ stoichiometry fired at 1400°C in H_2/N_2 and in which U was targeted as U^{3+} , the solid solution limit is at least 0.1 f.u. Our earlier dismissal of U^{3+} as a viable valence state[13] in the H_2/N_2 -fired material, on the basis of a very close similarity in the positions of the U L3 edge absorption edges in X-ray absorption spectroscopy measurements on the argon and H_2/N_2 –reduced samples, appears to be incorrect. The solid solubility limit of U on the Ca site of perovskite is ~ 0.25 f.u. on firing in H_2/N_2 . Note that $CaTiO_3$ is not substantially destabilised by such heating in a reducing atmosphere [14]. We believe that this result indicates U^{3+} is a viable valence state of U in an oxide system and is probably the first such observation (U^{3+} is a well-known entity in fluoride systems), though more measurements via spectroscopic methods such as X-ray photoelectron spectroscopy are necessary to check out this belief. Another possible system which clearly favors the occurrence of trivalent actinides is monazite[5] and we have made samples of a nominal UPO_4 composition in a reducing atmosphere to check this possibility; characterisation of this sample (supported by ANSTO) is underway.

Following earlier work [12], which did not include SEM, we fired samples of $\text{Ca}_{(1-x)}\text{U}_x\text{Ti}_{(1-2x)}\text{Al}_{2x}\text{SiO}_5$ titanite stoichiometry at 1300°C in argon and found only 0.02 f.u. of U in the titanite phase. Variations of the firing temperature in the range of 1200-1300°C did not lead to significantly different results.

U solubilities were studied in phosphate apatites of $\text{Ca}_9\text{Gd}_{0.33}\text{U}_{0.33}(\text{PO}_4)_5\text{SiO}_4\text{O}_2$ stoichiometry. Heating at 1300 or 1400°C in argon caused considerable decomposition of the apatite phase to form whitlockite, but the U incorporation in the apatite was ~ 0.5 f.u. Firing at 1200°C produced mainly apatite from XRD but did not produce grains of sufficient size for microanalysis.

Obviously U is a principal constituent of brannerite, but we have been able to show [15] that the substitution of Ca and rare earths in air- and Ar-fired brannerites produces U^{5+} in addition to U^{4+} by diffuse reflectance and X-ray absorption spectroscopy. U^{5+} was also identified in air-fired U-bearing zirconolites by these techniques [15]. Diffuse reflectance spectra also identified various absorption bands attributed to U^{4+} in samples where U was substituted on both Ca and Zr sites in zirconolite [16].

The substitution of U^{4+} in the Zr site of zirconolite produced the “normal” 2M polytype for substitutions up to 0.15 f.u., but further addition produced increasing amounts of the 4M polytype having a composition close to $\text{CaU}_{0.4}\text{Zr}_{0.6}\text{Ti}_2\text{O}_7$. Still further addition of U produced pyrochlore structures for more than about 0.7 f.u. of U, although the pyrochlore could not be made as a single phase [9]. Although $\text{CaThTi}_2\text{O}_7$ cannot be formed [17], presumably because the ionic size of Th is too large, CaUTi_2O_7 is clearly not unstable because of the ionic size of U^{4+} ; it can be formed in multi-phase systems.

Therefore the difficulty of forming 100% yields of CaUTi_2O_7 probably stems from the intrinsically poor solid state reactivity of UO_2 at temperatures of $\sim 1400^\circ\text{C}$.

4. GADOLINIUM AND HAFNIUM

The incorporation of Gd in the ceramic phases was known to be extensive for monazite, pyrochlore, zirconolite, perovskite and apatite, and that of Hf extensive in zircon, zirconolite, perovskite and pyrochlore, so the other phases were studied. The solid solubilities determined in the present work have been marked with an asterisk, and are shown in Table 2 below.

Table 2. Limits of Hf and Gd solid solubility in ceramic phases, in f.u.

Phase	Gd	Hf
Monazite (CePO_4)	1	< 0.01*
Pyrochlore ($\text{CaPuTi}_2\text{O}_7$)	2	2
Zirconolite ($\text{CaZrTi}_2\text{O}_7$)	1.4 [16]	1
Perovskite (CaTiO_3)	1	1
Apatite ($\text{Ca}_2\text{Nd}_8(\text{SiO}_4)_6\text{O}_2$)	8	<0.1*
Titanite (CaTiSiO_5)	0.3*	0.5*
Brannerite (UTi_2O_6)	0.5 [15]*	0.2 [15]*

* evaluated in present work

Gd substitutes in rare earth, actinide, and Ca or Zr sites; Hf substitutes in Ti, Zr or actinide sites

5. DISCUSSION AND CONCLUSIONS

We have defined at near subsolidus temperatures the solid solubilities for incorporating Pu, U, Gd and Hf in candidate nuclear waste ceramics. In nearly all cases, the host site for the desired substitution was obvious on the basis of ionic size similarities of the guest and host ions. It would be of interest to follow up on the experimental data to see whether a theoretical basis via lattice potentials and defect energies could be also be established. Charge compensation mechanisms were addressed where necessary. We are also conscious that there are several other phases that in 2001 may qualify as well-established candidate phases for nuclear waste incorporation; notably $\text{NaZr}_2(\text{PO}_4)_3$ (NZP) [18], fluorite, $\text{Th}_4(\text{PO}_4)_4\text{P}_2\text{O}_7$ [19], and zircon [20]. Zircon was not studied because it is relatively difficult to prepare insofar as sol-gel [21] or extensive ball-milling [22] methods are required.

Although ceramic brannerite has not been a candidate phase before 1997, its presence in the titanate ceramics selected for surplus Pu immobilisation have led to intensive study, at least at ANSTO.

We have obtained solid solubility limits of Pu, U, Hf and Gd in a variety of dry-fired candidate high-level waste ceramics at subsolidus temperatures generally in excess of 1200°C, and the heating was sufficiently prolonged to achieve near-equilibration at that temperature. The candidate phases were monazite, zirconolite, perovskite, pyrochlore, apatite, titanite and brannerite. In summary, apatite has low solubilities for tetravalent U and Pu, but has high solubility for Pu^{3+} ; it has high solubility for Gd, but not Hf. Titanite has low solubilities for tetravalent U and Pu, and the use of an argon firing

atmosphere did not greatly extend the Pu solubility; however solubilities for Hf and Gd were quite high. Monazite has high solubilities for Pu, U and Gd, but not Hf. Perovskite has limited solubilities for Pu and U in air, but in reducing atmospheres these solubilities are increased; and Hf and Gd have high solubilities. Zirconolite, pyrochlore and brannerite have appreciable or high solid solubilities for the actinides and the neutron absorbers.

Based on these data, it can be concluded that the easiest materials to deal with in the sense of standard ceramic fabrication in air or argon at reasonable temperatures (1200-1500°C), and high solid solubilities of Pu, U and the neutron absorbers Gd and Hf, are zirconolite, pyrochlore and brannerite. The cubic nature of pyrochlores reduces their tendency to crack when they experience radiation damage and several workers have noted that some zirconate-based pyrochlores do not amorphize after alpha-event irradiation. All phases considered here have considerable aqueous leach resistance.

6. REFERENCES

1. A. E. Ringwood, S. E. Kesson, K. D. Reeve, D. M. Levins and E. J. Ramm, in "Radioactive Waste Forms for the Future", Eds. W. Lutze and R. C. Ewing, Elsevier, Netherlands, 233-334 (1988).
2. E. R. Vance, R. A. Day, Z. Zhang, B. D. Begg, C. J. Ball and M. G. Blackford, J. Solid State Chem., 124, 77-82 (1996).
3. G.R. Lumpkin, K.L. Smith, M.G. Blackford, R. Gieré and C.T. Williams, Micron, 25, 581-7 (1994).
4. W. K. Kot, N. M. Edelstein, M. M. Abraham and L. A. Boatner, Phys. Rev. B 47, 3412 (1993).
5. C. J. Bjorklund, J. Amer. Chem. Soc., 79, 6347 (1958).
6. E. R. Vance, M. W. A. Stewart, R. A. Day, K. P. Hart, M. J. Hambley and A. Brownscombe, ANSTO Report R97m030 to Lawrence Livermore National Laboratory.
7. B. D. Begg, E. R. Vance and S. D. Conradson, J. Alloys and Compounds, 271-3, 221-8 (1998).
8. L. E. Russel, J. D. L. Harrison and N. H. Brett, J. Nucl. Mater., 2, 310 (1960).
9. M. W. Stewart, E. R. Vance, A. Jostsons, P. A. Walls, K. P. Hart, S. Moricca, R. A. Day, G. R. Lumpkin, C. J. Ball and D. S. Perera, ANSTO Report R00m031 to Lawrence Livermore National Laboratory.
10. F. W. Clinard, Jr., L. W. Hobbs, C. C. Land, D. E. Peterson, D. L. Rohr and R. B. Roof, J. Nucl. Mater. 105, 248 (1982).

11. G. J. McCarthy, J. G. Pepin and D. D. Davis, in Scientific Basis for Nuclear Waste Management, Volume 2, ed. C. J. M. Northrup (Plenum, New York and London), 297 (1979).
12. E. R. Vance and D. K. Agrawal, Nucl. Chem. Waste Manage., 3, 229 (1982).
13. E. R. Vance, M. L. Carter, B. D. Begg, R. A. Day and S. H. F. Leung, in Scientific Basis for Nuclear Waste Management XXIII, eds. R. W. Smith and D. W. Shoesmith, Materials Research Society, Pittsburgh, PA, USA, 431 (2000).
14. B. D. Begg, E. R. Vance, B. A. Hunter and J. V. Hanna, J. Mater. Res., 13, 3181 (1998).
15. E. R. Vance, J. N. Watson, M. L. Carter, R. A. Day, G. R. Lumpkin, K. P. Hart, Y. Zhang, P. J. McGlinn, M. W. A. Stewart and D. J. Cassidy, in Environmental Issues and Waste Management Technologies V, Eds. G. Chandler and X. Feng, American Ceramic Society, 561 (2000).
16. E. R. Vance, G. R. Lumpkin, M. L. Carter, C. J. Ball and B. D. Begg, J. Amer. Ceram. Soc., submitted for publication
17. R. A. McCauley and F. A. Hummel, J. Amer. Ceram. Soc., 33, 99-105 (1980).
18. R. Roy, L. J. Yang, J. Alamo and E. R. Vance, in Scientific Basis for Nuclear Waste Management VI, Ed. D. G. Brookins, North-Holland, Amsterdam, 15 (1983).
19. N. Dacheux, A. C. Thomas, B. Chassigneux, E. Pichot, V. Brandel and M. Genet, , in Scientific Basis for Nuclear Waste Management XXII, Eds. D. J. Wronkiewicz and J. H. Lee, Materials Research Society, Pittsburgh, PA, USA, 85 (1999).
20. R. C. Ewing and W. Lutze, J. Mater. Res., 10, 243 (1995).
21. R. C. Ewing and R. F. Haaker, J. Amer. Ceram. Soc, 64, C-149 (1981).

22. D. R. Spearing and J. Y. Huang, J. Amer. Ceram. Soc., 81, 1964 (1998).

7. PRESENTATIONS AND PAPERS ON EMSP PROJECTS

PRESENTATIONS

1. X. Feng, H. Li, L. L. D. L. Li, J. G. Darab, M. J. Schweiger, J. D. Vienna, B. C. Bunker, P. G. Allen, J. J. Bucher, I. M. Craig, N. M. Edelstein, D. K. Shuh, R. C. Ewing, L. M. Wang and E. R. Vance, Distribution and Solubility of Radionuclides in Waste Forms for Disposition of Plutonium and Spent Nuclear Fuels: Preliminary Results, American Ceramic Society Annual Meeting, Cincinnati, April, 1998.
 2. E. R. Vance, M. L. Carter, J. N. Watson, R. A. Day and S. Leung, Crystal chemistry and Synthesis of Pyrochlore Structured CaATi_2O_7 and Brannerite, ATi_2O_6 (A = Ce, U, Th, Pu) Phases for Pu Immobilisation, 23rd Annual Australian Institute of Physics Condensed Matter Meeting, Wagga Wagga, NSW, Australia, Feb. 3-5 (1999).
 3. E. R. Vance, J. N. Watson, M. L. Carter, R. A. Day, G. R. Lumpkin, K. P. Hart, Y. Zhang, P. J. McGlinn, M. W. A. Stewart and D. J. Cassidy, Crystal chemistry, radiation effects and aqueous leaching of brannerite, UTi_2O_6 , American Ceramic Society Annual Meeting, Indianapolis, April 28, 1999.
 4. E. R. Vance, M. L. Carter, B. D. Begg and S. H. F. Leung, Solid Solubilities of Pu, U, Hf and Gd in Candidate Ceramic Phases for Actinide Waste Immobilisation, Annual Meeting of the Materials Research Society, Boston, MA, USA, Nov. 29 - Dec. 3, 1999.
- M. James, J. N. Watson and E. R. Vance, Structures of Brannerite, Condensed Matter Meeting XXIV, AIP, Wagga Wagga, NSW, Australia, 1-4 Feb., 2000.

5. E. R. Vance, M. Colella, K. L. Smith, G. R. Lumpkin, M. L. Carter, B. D. Begg and G. J. Thorogood, Vacancies and Structures of Zirconolites and Defect Titanate Pyrochlores, Condensed Matter Meeting XXIV, AIP, Wagga Wagga, NSW, Australia, 1-4 Feb., 2000.
6. D. M. Strachan, J. G. Darab, L. L. Davis, H. Li, L. Li, M. Qian, D. L. Caulder, P. G. Allen, C. H. Booth, J. J. Bucher, N. M. Edelstein, P. Liu, W. W. Lukens, D. K. Shuh, R. C. Ewing, D. Zhao and E. R. Vance, Solubility and Solution Mechanisms for Actinides and Neutron Absorbers in Amorphous and Crystalline Waste Forms, EMSP Workshop, Atlanta, GA, April 24, 2000.
7. E. R. Vance, K. L. Smith, G. R. Lumpkin, B. D. Begg, C. J. Ball, and J. H. Hadley, Jr. Cation Vacancies in Titanate Phases, Austceram, Sydney, Australia, June 25-27, 2000.

PUBLICATIONS

1. E. R. Vance, M. L. Carter, B. D. Begg, R. A. Day and S. H. F. Leung, Solid Solubilities of Pu, U, Hf and Gd in Candidate Ceramic Phases for Actinide Waste Immobilisation, Mat. Res. Soc. Symp. Proc. Vol. 608, Ed. R. W. D. W. Shoesmith, Materials Research Society, Pittsburgh, PA, USA, 431-6 (2000).
2. E. R. Vance, J. N. Watson, M. L. Carter, R. A. Day, G. R. Lumpkin, K. P. Hart, Y. Zhang, P. J. McGlinn, M. W. A. Stewart and D. J. Cassidy, Crystal chemistry, radiation effects and aqueous leaching of brannerite, UTi_2O_6 , in Environmental Issues and Waste Management Technologies V, Eds. G. Chandler and X. Feng, American Ceramic Society, 561-8 (2000).
3. E. R. Vance, J. N. Watson, M. L. Carter, R. A. Day and B. D. Begg, Crystal chemistry and Stabilization in Air of Brannerite, UTi_2O_6 , J. Amer. Ceram. Soc., 84, 141-4 (2001).
4. E. R. Vance, G. R. Lumpkin, M. L. Carter, C. J. Ball and B. D. Begg, The Incorporation of U in Zirconolite ($CaZrTi_2O_7$), about to be submitted to J. Amer. Ceram. Soc.
5. E. R. Vance, M. L. Carter, R. A. Day and B. D. Begg, Solubilities of different U valences in perovskite, $CaTiO_3$, in preparation
6. E. R. Vance, K. L. Smith, G. R. Lumpkin, B. D. Begg, C. J. Ball, and J. H. Hadley, Jr., Cation Vacancies in Titanate Phases, in preparation.
6. E. R. Vance, M. L. Carter, R. A. Day and C. J. Ball, Plutonium Incorporation in Silicate Apatite, in preparation

CRYSTAL CHEMISTRY, RADIATION EFFECTS AND AQUEOUS LEACHING OF BRANNERITE, UTi_2O_6

E.R. Vance, J N. Watson, M.L. Carter, R.A. Day, G.R. Lumpkin, K.P. Hart, Y. Zhang, P.J. McGlinn, M.W.A. Stewart and D.J. Cassidy, Materials Division, ANSTO, Menai, NSW 2234, Australia

ABSTRACT

Pure brannerite, UTi_2O_6 , can be formed only under low oxygen pressures by dry ceramic processing techniques, but the substitution of ~ 0.3 formula units of Ca or Gd for U allows the stabilisation of the phase in air. The stabilisation mechanism for Ca/Gd in air-fired UTi_2O_6 appears to be the formation of U valence states $> +4$. Absorption bands near 1500 nm in both air- and Ar-fired U-brannerite doped with Ca and Gd were observed using diffuse reflectance spectroscopy and attributed to U^{5+} . Other ionic substitutions involved Hf and Zr for U, Gd + Nb \leftrightarrow U + Ti, and Fe in the Ti site. DTA showed the radiation damage in an X-ray amorphous natural sample to anneal on heating, giving peaks in the 500-1000°C range. The stored energy in the amorphous brannerite was evaluated as > 15 kJ/mole. The density change accompanying amorphisation is 5-10%. The 70°C aqueous leach rate of synthetic UTi_2O_6 was a minimum at pH ~ 7 and had a value of $\sim 10^{-4}$ g/m²/day.

INTRODUCTION

Brannerite is a mineral which has attracted recent interest as a minor phase in titanate-based ceramics of the Synroc¹ type designed for the geological immobilisation of excess weapons Pu^{2,3}. Brannerite in the ceramics was found to incorporate neutron absorbers such as Gd and Hf in its structure as well as Pu and U. The crystal structure is monoclinic^{4,5} and both the U and Ti are in distorted octahedral co-ordination.

The crystal chemistry of brannerite is of interest for (a) what elements stabilise brannerite in air-fired ceramics, since pure UTi_2O_6 made by dry ceramic techniques is stable under only low oxygen pressures⁵; (b) the solid solubility limits of neutron absorbers such as Gd and Hf; and (c) what impurity elements in general can be taken up by brannerite. Other important questions for the radioactive waste immobilisation application are the aqueous dissolution behaviour and radiation damage resistance of brannerite.

EXPERIMENTAL

Samples were made by the alkoxide/nitrate route⁶, except that Hf was used as the oxide. Mixtures were dried and then calcined in argon or air at 750°C for 1 h. The calcines were wet-milled for 16 hr and dried. Samples were mostly prepared by cold-pressing calcines and firing the pellets at 1350-1450°C.

Scanning electron microscopy (SEM) was carried out with a JEOL 6400 instrument run at 15 kV, and fitted with a NORAN Instrument Voyager IV X-ray microanalysis System (EDS) which utilised a comprehensive set of standards for quantitative work⁷. X-ray diffraction (XRD) was performed with a Siemens D500 instrument employing Co $K\alpha$ radiation. Transmission electron microscopy (TEM) was carried out with a JEOL 2000FXII instrument equipped with a Link energy-dispersive X-ray detector. The microscope was operated at 200 kV and calibrated for electron diffraction work using a gold standard. Energy-dispersive analyses were carried out using the calibration and operating procedures previously developed for natural zirconolite samples⁸.

Diffuse reflectance spectroscopy (DRS) was carried out on finely powdered samples with a Cary 5 device over the 300 - 2000 nm range.

Differential thermal and thermogravimetric analysis were carried out in an Ar atmosphere at temperatures up to 1300°C in a Setaram instrument, using alumina as a standard and a ramp rate of 5°C/min. The sample was thermally cycled twice, with the second cycle giving an indication of the instrumental baseline.

Leaching measurements at 70°C were made by a flow-through method (12 mL/day) on < 150 µm powdered hot-pressed UTi₂O₆.

RESULTS AND DISCUSSION

Preparation of UTi₂O₆

Other than simply sintering in argon containing < 10 ppm of O₂, appropriate redox conditions were found to correspond to the addition of 2 wt% of Ti metal powder to a calcine produced in argon, sealing inside a stainless steel bellows and hot-pressing in a graphite die at 1200°C/20MPa for 2 h. This gave essentially full density, rather than the 70-90% of the theoretical value routinely achievable with pressureless sintering. However the ~ 100 µm-thick brannerite surface layer contained mainly U and Ti oxides and was removed mechanically. As well as stoichiometric preparations, materials containing 5 wt% excess TiO₂ or UO₂ were fabricated, and from SEM measurements, the U/Ti stoichiometry of the brannerite phase was unchanged within the experimental accuracy of ~ 0.02 formula units. The extra phases were rutile or UO₂.

Stabilisation of U-brannerite in air atmospheres

Since the baseline ceramic for Pu immobilisation yielded brannerite after sintering in air³, other oxides present (Ca, Gd, Hf, Pu) in this ceramic were responsible for its stabilisation. But although these ions were substituted for some of the U, there were no obvious micro-analytical differences in the (minority) brannerite phases in the baseline ceramic formed in air and argon sintering atmospheres. The substitution of Gd or Ca for U could be charge compensated by (a) the formation of higher U valences, +5 or +6, or (b) oxygen deficiency. To investigate these possibilities, ceramics of U_(1-x)(Ca/Gd)_xTi₂O_{6-y} stoichiometries were formulated and fired in air and argon.

Ca additions: U_(1-x)Ca_xTi₂O_{6-y}: For x = 0.1 and 0.2, samples fired in air yielded mixtures of brannerite (U_{0.77}Ca_{0.23}Ti_{2.1}O₆), U₃O₈ and rutile. For x = 0.5, we obtained ~ 40% of brannerite (U_{0.73}Ca_{0.29}Ti_{2.1}O₆), plus pyrochlore (Ca_{1.5}U_{0.8}Ti_{1.9}O₇) and rutile. Argon-fired materials produced brannerites having essentially the starting composition for x = 0.1 and 0.2. For x = 0.5, the phases present were brannerite (U_{0.8}Ca_{0.2}Ti_{2.1}O₆), pyrochlore (Ca_{1.2}U_{0.8}Ti_{2.1}O₇) and rutile. These results indicated limiting Ca solubilities of ~ 0.2 and 0.3 formula units in argon- and air-fired materials respectively.

To obtain information on the U valences, DRS measurements were made on stoichiometric UTi₂O₆, and U_{0.74}Ca_{0.26}Ti₂O₆ (nominal composition) fired in air or argon. U⁴⁺ gives absorption peaks through the range of 400-2000 nm, but U⁵⁺ yields peaks only in the 1000-1500 nm range⁹. No absorption peaks were observed for pure brannerite, but the argon- and air-fired Ca-doped samples both yielded a peak at 1448 nm, with possibly a weak extra peak near 1670 nm-see Fig. 1. The discontinuity near 800 nm in Fig. 1 is due to a detector change. In the pure brannerite, the absence of absorption peaks suggests that there are no isolated U⁴⁺ ions. The weak absorption peaks at 1448 and possibly 1670 nm in the Ca-doped samples are attributed to relatively isolated U⁵⁺. Green fluorescence characteristic of U⁶⁺ was not observed in either the air- or argon-fired samples upon ultraviolet irradiation. The limiting solubility of Ca with all the U existing as U⁵⁺, would correspond to U_{0.67}Ca_{0.33}Ti₂O₆, a composition close to the observed limiting Ca solubility in air-fired material.

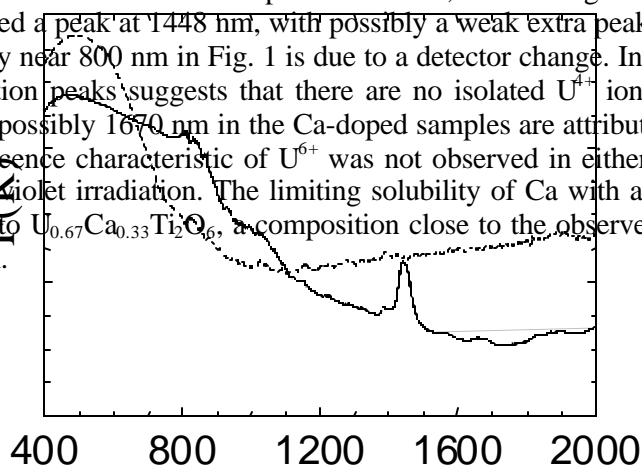


Figure 1. DRS spectrum(absorbance units) showing peak at 1450 nm in Ca-doped sample, with no corresponding peak in pure UTi_2O_6

Gd additions: $\text{U}_{1-x}\text{Gd}_x\text{Ti}_2\text{O}_{6-z}$: Single-phase brannerites of the starting compositions were obtained for $x = 0.1$ and 0.2 after firing in argon, but for $x = 0.5$, only $\sim 60\%$ of the sample consisted of brannerite ($\text{U}_{0.55}\text{Gd}_{0.45}\text{Ti}_{2.1}\text{O}_6$) with the rest being pyrochlore ($\text{Gd}_{1.69}\text{U}_{0.08}\text{Ti}_{2.15}\text{O}_7$) and rutile. When fired in air, the $x = 0.1$ and 0.2 brannerites contained ~ 0.32 formula units (f.u) of Gd; other phases were U_3O_8 and rutile. The $x = 0.5$ sample fired in air was almost single phase ($\text{U}_{0.52}\text{Gd}_{0.48}\text{Ti}_{2.1}\text{O}_6$) and corresponds to the limiting value of $\text{U}_{0.5}\text{Gd}_{0.5}\text{Ti}_2\text{O}_6$ if all the U is present as U^{5+} . DRS on the $x = 0.2$ samples fired in air or argon yielded similar results to the Ca-doped samples (see Fig. 1) and no ultraviolet-induced fluorescence was observed.

Ca and Gd solubility in ThTi_2O_6

The solubilities of Ca and Gd in ThTi_2O_6 (isostructural with brannerite) in which actinide valence states $> 4+$ cannot be present were studied. The solubility of Ca was found to be very small (< 0.01 f.u.); extra phases were rutile and Ca- or Gd-doped perovskite with the reaction in the first instance being: $\text{Th}_{(1-x)}\text{Ca}_x\text{Ti}_2\text{O}_6 \rightarrow (1-x)\text{ThTi}_2\text{O}_6 + x\text{CaTiO}_3 + x\text{TiO}_2$. However some solubility of Th in the perovskite phase was apparent ($\text{Ca}_{0.78}\text{Th}_{0.11}\square_{0.11}\text{TiO}_3$), where the \square is a Ca vacancy required to effect overall charge neutrality. The solubility of Gd in the brannerite structure was measured as 0.1 f.u., with the formation of additional Th-doped pyrochlore. Here the reaction can be written in the first instance as:

$\text{Th}_{(1-x)}\text{Gd}_x\text{Ti}_2\text{O}_6 \rightarrow (1-x)\text{ThTi}_2\text{O}_6 + (x/2)\text{Gd}_2\text{Ti}_2\text{O}_7 + x\text{TiO}_2$. However as mentioned above, there was restricted solubility of Gd in the Th-brannerite, and Th solubility in the pyrochlore, with the composition of the pyrochlore in the $x = 0.2$ material being given by approximately $\text{Gd}_{1.5}\text{Th}_{0.25}\text{Ti}_2\text{O}_7$.

Thus as expected from the theory advanced above, i.e. there are additional charge compensation mechanisms available in U-brannerite via U valence states $> +4$, relative to Th-brannerite, the solubilities of Gd and Ca in the Th-brannerite are much smaller than those in U-brannerite. However the solubility of Gd in ThTi_2O_6 may well involve oxygen deficiency and neutron diffraction measurements will be useful to examine this possibility. The departure of the Ti stoichiometry from 2 f.u. in both the Ca- and Gd-doped brannerites will be investigated further.

Other ions in brannerite

Other ions contained in natural brannerites include Nb and $\text{Fe}^{4-6,10}$, so these were explored in synthetic materials. Hf was of interest as neutron absorber and Ce as a simulant of Pu. Pu was of interest in its own right.

Hf: U was substituted with 0.1 , 0.2 or 0.5 f.u. of Hf, and the samples were sintered in argon. Though the more dilute samples were not entirely single-phase, SEM showed that the brannerite compositions were close to the starting compositions. The $\text{U}_{0.5}\text{Hf}_{0.5}\text{Ti}_2\text{O}_6$ sample showed that 0.24 f.u. of Hf could be incorporated in the brannerite, with ~ 30 wt% of the sample consisting of U-doped HfTiO_4 ($\text{Hf}_{0.84}\text{U}_{0.11}\text{Ti}_{1.05}\text{O}_4$), and additional rutile ($\text{Hf}_{0.82}\text{U}_{0.01}\text{Ti}_{0.82}\text{O}_2$). Broadly similar results were obtained with non-radioactive analogue $\text{Ce}_{(1-x)}\text{Hf}_x\text{Ti}_2\text{O}_6$ brannerite-structured compounds sintered in air. Complete substitution was found for $x = 0.1$ and 0.2 , and the saturation loading of Hf corresponded to $x = 0.22$, a value very similar to that determined for the U-brannerite.

Zr: Samples of $\text{U}_{0.76}\text{Zr}_{0.24}\text{Ti}_2\text{O}_6$ stoichiometries were fired in argon and air. No brannerite was found in the air-fired material, only U_3O_8 , rutile and ZrTiO_4 . For the argon sinter, brannerite ($\text{U}_{0.8}\text{Zr}_{0.2}\text{Ti}_2\text{O}_6$) was the major phase, with some UO_2 and rutile also being present.

Gd-Nb: Coupled Gd, Nb substitutions were tried according to $U_{(1-x)}Gd_xTi_{(2-x)}Nb_xO_6$ stoichiometries using argon as the sintering atmosphere. For $x = 0.1$ and 0.2 , the brannerites were largely single phase, of the designated compositions. However for $x = 0.5$, the sample was multi-phase; the brannerite composition was given by $Gd_{0.67}U_{0.29}Ti_{1.29}Nb_{0.72}O_6$ and the other oxide phases had compositions of $U_{0.77}Gd_{0.01}Ti_{0.18}Nb_{2.03}O_7$ and $U_{0.64}Gd_{0.07}Ti_{0.53}Nb_{1.82}O_7$.

Fe: Samples with Fe nominally substituted for 0.2 or 0.4 f.u. of Ti were produced by firing in air and argon. In air, Fe-substituted brannerite having a composition of about $U_{1.00}Ti_{1.60}Fe_{0.49}O_6$ was formed, together with U_3O_8 and rutile. The argon-fired samples yielded almost single phases with the nominated brannerite compositions formed.

Pu: Only ~ 50% yield of the brannerite phase was obtained on heating at 1500°C for 16 h in air, with the yield after heating at 1400°C being close to zero. After firing at 1525°C for 16 h, the yield increased to ~ 75 %. In each case, the additional phases were PuO_2 and TiO_2 .

Natural brannerites

EDS analyses obtained by SEM demonstrate that the major impurity elements in unaltered natural brannerites are Ca, rare earth elements (REE = Y plus the lanthanides), Th, and Pb. Preliminary results indicate that these elements are present in variable amounts, ranging from values below detection up to maximum values of 0.45 Ca, 0.15 REE, 0.20 Th, and 0.10 Pb atoms per formula unit. Other minor elements were detected in some of the natural samples, including Si, Fe, Ni, and Nb. Of this group, we found maximum concentrations of 0.10 Si, 0.10 Fe, and 0.05 Nb atoms per formula unit.

TEM showed that all samples were amorphous due to alpha-decay damage^{4-6,10}. Electron diffraction patterns typically consist of two diffuse rings with equivalent d-spacings of approximately 3.1Å and 1.9Å, similar to many metamict (amorphous) oxide and silicate minerals¹¹. Some of the grains examined thus far also exhibit weak diffraction spots. The diffraction spots appear to be due to the presence of fine grained (10-50 nm) inclusions of another phase which is yet to be identified. TEM results also show that some of the brannerite grains also contain 10-200 nm spherical voids, similar to previous observations on metamict zirconolite¹¹.

Table 1. Localities, evidence for alteration, and TEM data for natural brannerite.

Locality	Age (Ma)	Host rock type	Alteration	Dose (α /mg)*
South Australia	1580	granite	heavy	1.7×10^{18}
Cordoba, Spain	> 400	ore deposit	minor	$> 6 \times 10^{17}$
Ticino, Switzerland	> 30	granite	moderate	$> 3 \times 10^{16}$
W. Province, Zambia	> 200	ore deposit	minor	$> 2 \times 10^{17}$
California	> 65	quartz veins	moderate	$> 7 \times 10^{16}$
Bou-Azzer, Morocco	> 100	quartz veins	minor	$> 1 \times 10^{17}$
Stanley, Idaho	> 30	placer deposit	minor	$> 3 \times 10^{16}$

*All samples are fully amorphous (metamict) at the stated dose.

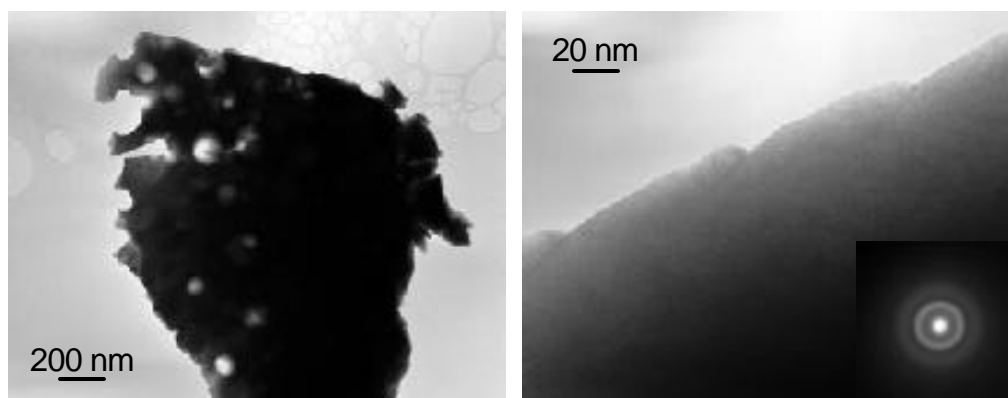


Figure 2. TEM results for unaltered brannerite. Left: bright field image shows presence of voids in some grains. Right: bright field image and diffraction pattern (inset) illustrate the fully amorphous (metamict) structure.

Other workers^{4-6,10} have noted that natural brannerites are normally X-ray amorphous, but that on heating to 600-1000°C in an unspecified atmosphere (presumably air) they recrystallise. Given the instability in air of the UTi_2O_6 end-member, this seemed surprising, but natural samples (see above and refs. 4-6, 10) show the presence of several percent of rare earths and Ca, which favour stabilisation of the structure in air.

DTA/TGA results for an argon atmosphere are shown for the Spanish brannerite. The weight losses may derive from OH^- -bearing impurities. From comparative measurements using the heat of fusion of pure Au, it was determined that the stored energy accompanying the metamict-crystalline transition was ~ 15 kJ/mole taking the areas under the exothermic peaks at 535 and 669°C. XRD after heating in argon for 2 h at 500, 700, 900, 1100 and 1300°C showed however that the major recrystallisation took place between 900 and 1100°C, so the stored energy calculated above is a severe underestimate: a better value could not confidently be derived from the DTA curve because the exotherm is evidently too broad, and reduced by endothermic effects associated with weight losses. The Archimedes' density of another 3 g piece of the Spanish sample decreased gradually from 5.0 (unheated) to 4.8 g/cm³ on heating at 500-900°C, before increasing to 5.2 g/cm³ after heating at 1100 and 1300°C.

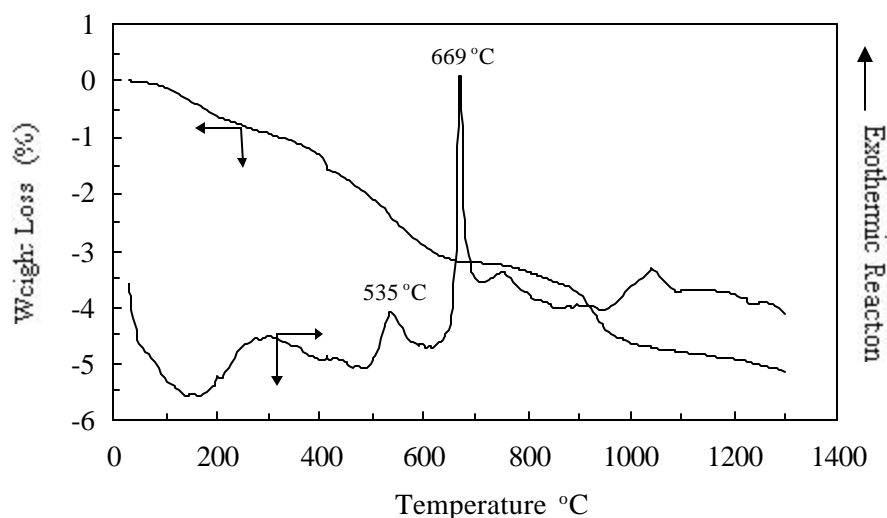


Figure 3. DTA/TGA results for natural Spanish brannerite. DTA baseline approximately flat, but influenced by $\sim 5\%$ weight loss during the first heatup.

Leaching of synthetic brannerites

The flow-through tests were carried out using the following aqueous media: 0.05M KH phthalate + 0.05M HCl (pH = 2.1); 0.05M H₃BO₃ + 0.004M NaOH (pH = 7.9); and 0.05M H₃BO₃ + 0.044 M NaOH (pH = 9.8). Leachates were sampled initially daily and later, twice a week. The leachates were acidified to 3% HNO₃ by volume and analysed by inductively coupled plasma-mass spectrometry for U and Ti. The leach rates are shown in Fig. 4. Initially the variations of leach rate with pH were of order 10³, but after 60 days the difference had narrowed to ~ 10². The leach rates at longer times were relatively constant, with the lowest U release of ~ 10⁻⁴ g/m²/d occurring at pH = 7.9. Even samples leached for 60 days in the pH = 2.1 medium showed no visible signs of corrosion by SEM. The Ti release rates were lower than those of U, and had values of ~ 5 x 10⁻³ g/m²/d at pH = 2.1 and < 3 x 10⁻⁵ g/m²/d for the higher pHs (below detection limits).

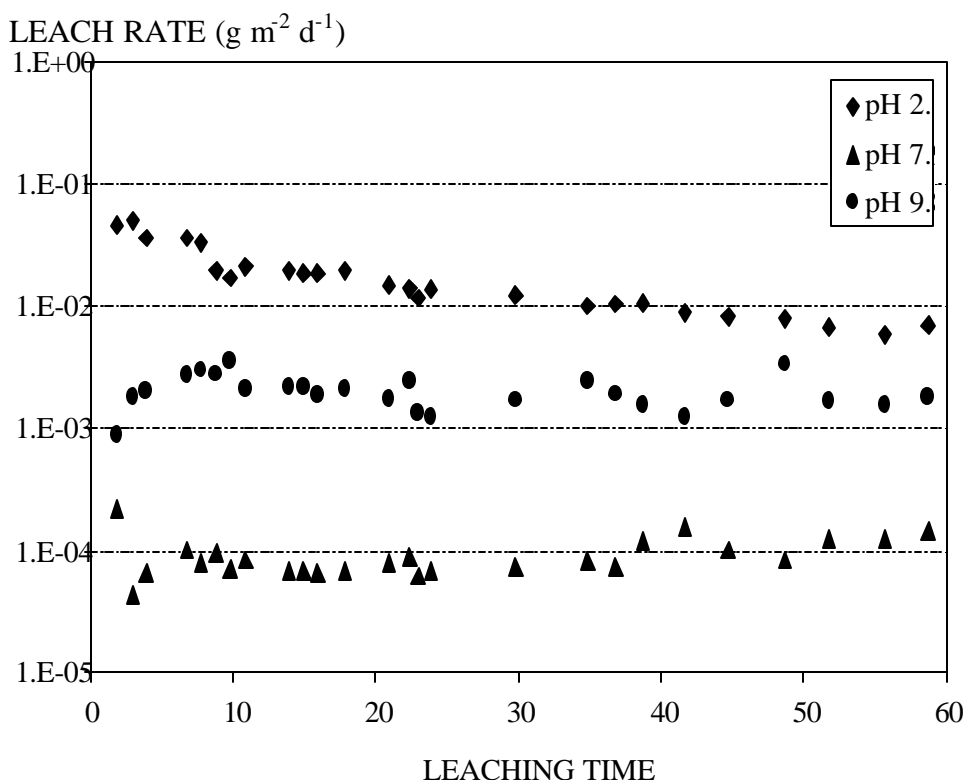


Figure 4. Normalised U leach rates measured from U-brannerite at 70°C and 12 ml/d.

CONCLUSIONS

Ca and rare earths can be extensively substituted for U in brannerite, leading to U⁵⁺ in addition to U⁴⁺, as shown by diffuse reflectance spectroscopy. The substitutions of Ca and rare

earths for U increase the oxygen activity at which brannerite is stable. Other substitutions, such as Hf/Zr for U, $Gd^{3+} + Nb^{5+}$ for $U^{4+} + Ti^{4+}$, Fe for Ti, are also possible. The major impurities in natural brannerites are rare earths, Ca and Pb. Radiation damage annealing over the 500-1000°C range was demonstrated by DTA for a natural sample and the derived value of the stored energy accompanying metamictisation was > 15 kJ/mole. The change of density for the crystalline-metamict transition was found as 5-10 %. Leaching of synthetic brannerite was observed to be a minimum near pH ~ 7 , with a value of $\sim 10^{-4}$ g/m²/day at 70°C, based on U extraction.

ACKNOWLEDGEMENTS

This work was supported in part by the Environmental Management Science Program of the US Department of Energy and partly by the Lawrence Livermore National Laboratory. We wish to thank S. Thomson and V. Luca for help with the diffuse reflectance spectroscopy, E. Loi for the ICP-MS analyses, A. Brownscombe for preparing the Pu-doped samples, and B. Ebbinghaus, M. James and D. Strachan for helpful discussions.

REFERENCES

- ¹A.E. Ringwood, S.E. Kesson, N.G. Ware, W. Hibberson and A. Major, "Immobilisation of High Level Nuclear Wastes in SYNROC", *Nature (London)* 278, 219-23 (1979).
- ²B.B. Ebbinghaus, R.A. VanKonynenburg, F.J. Ryerson, E.R. Vance, M.W.A. Stewart, A. Jostsons, J.S. Allender, T. Rankin and J. Congdon, "Ceramic Formulation for the Immobilization of Plutonium", *Waste Management '98* (CD-ROM), Tucson, AZ, USA, March 5, 1998.
- ³E.R. Vance, M.W.A. Stewart, R.A. Day, K.P. Hart, M.J. Hambley and A. Brownscombe, "Pyrochlore-rich Titanate ceramics for Incorporation of Plutonium, Uranium and Process Chemicals", ANSTO report (1997).
- ⁴J.T. Szymanski and J.D. Scott, "A crystal-structure refinement of synthetic brannerite, UTi_2O_6 , and its bearing on rate of alkaline-carbonate leaching of brannerite", in ore, *Canad. Mineral.*, 20, 271-9 (1982).
- ⁵J.E. Patchett and E.W. Nuffield, "Studies of radioactive compounds. X. The synthesis and crystallography of brannerite", *Canad. Mineral.*, 6, 483-90 (1960).
- ⁶A.E. Ringwood, S.E. Kesson, K.D. Reeve, D.M. Levins and E.J. Ramm, "Synroc", in *Radioactive Waste Forms for the Future*, Eds. W. Lutze and R.C. Ewing, Elsevier, 233-334 (1988).
- ⁷E.R. Vance, R.A. Day, Z. Zhang, B. D. Begg, C.J. Ball and M.G. Blackford, "Charge Compensations in Gd-doped $CaTiO_3$ ", *J. Solid State Chem.*, 124, 77-82 (1996).
- ⁸G.R. Lumpkin, K.L. Smith, M.G. Blackford, R. Gieré and C.T. Williams, "Determination of 25 elements in the complex oxide mineral zirconolite by analytical electron microscopy", *Micron*, 25, 581-7 (1994).
- ⁹E.R. Vance and D.J. Mackey, "Optical studies of U^{4+} and U^{5+} in zircon, hafnon and thorite", *Phys. Rev.B*, 18, 185-90 (1978).
- ¹⁰A. Pabst, "Brannerite from California", *Amer. Mineral.*, 39, 109-17 (1954).
- ¹¹R.C. Ewing and T.J. Headley, "Alpha-recoil damage in zirconolite ($CaZrTi_2O_7$)", *J. Nucl. Mater.*, 119, 102-9 (1983).

CRYSTAL CHEMISTRY AND STABILIZATION IN AIR OF BRANNERITE, UTi_2O_6

E.R. Vance, J N. Watson, M.L. Carter, R.A. Day and B. D. Begg, ANSTO, Menai, NSW
2234, Australia

ABSTRACT

Brannerite, UTi_2O_6 , can be formed only under low oxygen pressures by dry ceramic processing techniques, but the substitution of ~ 0.2 and 0.3 formula units (f.u.) of Ca or Gd respectively for U allows the stabilisation of the phase in air. The Ca/Gd in brannerite provides charge compensation for some U to exist in valence states $> +4$, as found by X-ray absorption spectroscopy of the U L3 edge. The maximum solubilities of Ca and trivalent rare earths in the air-fired samples, 0.3 and 0.5 f.u. respectively, correspond to U having an average valence of $+5$. Ca and Gd had maximum solubilities of 0.2 and 0.45 f.u. respectively in argon-fired samples. An absorption band at 1448 nm in both air- and Ar-fired U-brannerite doped with Ca and Gd was observed using diffuse reflectance spectroscopy and attributed to an electronic transition of U^{5+} . A similar band was observed in an annealed natural brannerite, which contained Ca, rare earths and Th, although the band was present at ~ 1520 nm in the unannealed, X-ray amorphous sample. In synthetic ThTi_2O_6 (thorutite, having the brannerite structure), the solubility of Ca was undetectable and that of rare earths < 0.1 f.u. Other ionic substitutions in synthetic brannerites involved Hf, Pu, La, and Y for U, (Gd + Nb) for U + Ti, and Fe in the Ti site.

I. Introduction

Brannerite, nominally UTi_2O_6 , is a mineral which is nearly always X-ray amorphous because of radiation damage from alpha-decay of U, Th and daughter isotopes, but it can be recrystallised by heating to temperatures in the vicinity of 1000°C . It is known to incorporate rare earth, Ca and Th impurities in its structure. The crystal structure is monoclinic[1,2] and both the U and Ti are in distorted octahedral co-ordination. Brannerite is a minor phase in the Synroc[3]-based pyrochlore-rich ceramics designed for the geological immobilisation of excess US weapons Pu[4,5]. In these ceramics the brannerite was found to incorporate Pu together with neutron absorbers such as Gd and Hf, as well as U. The neutron absorbers are present to overcome potential criticality problems associated with the presence of Pu. It was clear from the chemical composition of the brannerite phase in these ceramics[4,5] that Ca, Hf, Gd and Pu all substituted into the actinide site and little difference in the brannerite composition was found between the ceramics fired in argon or air. Since pure UTi_2O_6 can only be synthesised by dry ceramic techniques under low-oxygen conditions [1], it was clear that stabilisation of brannerite in the air-fired ceramics was due to the incorporation of the impurity ions. Preliminary work[6] had also shown that partial Ca and Gd substitutions for U allowed the stabilisation of brannerite in air.

The present work deals with finding (a) the limits of Ca and Gd substitutions for U which stabilise brannerite in air atmospheres and investigating possible mechanisms for charge compensation and (b) which impurity elements in general can be taken up by synthetic brannerite.

II. Experimental

Samples were made by the alkoxide/nitrate route [7], except that Hf was added as the oxide. Mixtures were dried and then calcined in argon or air at 750°C for 1 h. The calcines were wet-milled for 16 h and dried. Samples were prepared by cold-pressing calcines and firing the pellets at 1350-1450°C, generally for 14 h in either argon or air.

Scanning electron microscopy (SEM) was carried out with a JEOL 6400 instrument run at 15 kV, and fitted with a Tracor Northern TN5502 energy-dispersive spectrometer (EDS), which utilised a comprehensive set of standards for quantitative work [8]. X-ray diffraction (XRD) was performed with a Siemens D500 instrument employing Co K α radiation.

The detection of electronic absorption bands from the brannerites in the visible and infrared sections of the electromagnetic spectrum, can in principle characterise different U valences in the samples. Single crystal samples are preferred for this purpose, but in their absence, diffuse reflectance spectroscopy (DRS) was carried out on flat surfaces of finely powdered samples with a Cary 5 instrument over the 300 - 2000 nm range. The raw data were transformed to Kubelka-Munk absorption vs. wavelength plots.

X-ray absorption data to probe U valences were obtained on beam line 4-2 at the Stanford Synchrotron Research Laboratory. UTi_2O_6 and CaUO_4 were used as valence standards (+4 and +6 respectively).

III. Results and Discussion

(1) Ceramic Preparation of UTi_2O_6

Simply sintering the correct stoichiometry in argon containing < 10 ppm of O_2 , at $\sim 1300^\circ C$ produced single-phase, but porous brannerite (sintering in air produced $U_3O_8 + TiO_2$). The preparation of dense brannerite required the addition of 2 wt% Ti metal powder to a powder of UTi_2O_6 stoichiometry calcined in argon, sealing inside a stainless steel bellows and hot-pressing in a graphite die at $1250^\circ C/20 MPa$ for 2 hr. This gave essentially full density, rather than the 70-90% of the theoretical value routinely achievable with the pressureless sintering. The purpose of the Ti metal powder was to optimise the redox conditions for brannerite formation, although minor reduced Ti oxide was present also. As well as stoichiometric preparations, in which SEM showed that the Ti/U atomic ratio was 2.00 ± 0.04 , materials containing 5 wt% excess TiO_2 or UO_2 were fabricated. From SEM measurements, the Ti/U stoichiometry of the brannerite phase in these materials was unchanged within the experimental accuracy of ~ 0.02 formula units. The extra phases were rutile or UO_2 when the excess TiO_2 or UO_2 respectively were present.

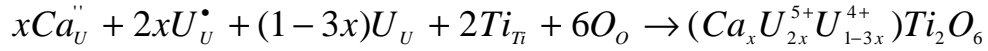
(2) Stabilisation of Ca/Gd-doped U-brannerite in air atmospheres

Brannerite may be stabilised in an air atmosphere at high temperatures by partial substitution of Gd or Ca for U [6]. This would imply that either (a) the partial substitution of Ca/Gd for U charge compensates for U valence states $> +4$ or (b) that brannerite is

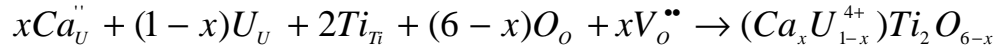
stabilised by the presence of oxygen vacancies. These possibilities may be represented in Kroger-Vink notation as:



for x formula units of hexavalent U compensated by an equivalent amount of Ca substituted on the U site. Also,



for x formula units of pentavalent U compensated by an appropriate amount of Ca substituted on the U site. Finally,



for Ca-substituted brannerite stabilised by the presence of oxygen vacancies.

To investigate these possibilities, ceramics of $U_{(1-x)}(Ca/Gd)_xTi_2O_{6-y}$ stoichiometries were formulated and fired in air and argon.

Ca additions: $U_{(1-x)}Ca_xTi_2O_{6-y}$: For x = 0.1 and 0.2, samples fired in air yielded mixtures of brannerite ($U_{0.77}Ca_{0.23}Ti_2O_6$), U_3O_8 and rutile, although the x = 0.2 sample was closer to forming single-phase brannerite. For x = 0.5, we obtained brannerite ($U_{0.73}Ca_{0.29}Ti_2O_6$), plus pyrochlore-structured $Ca_{1.5}U_{0.8}Ti_{1.9}O_7$ and rutile. Argon-fired materials produced brannerites having essentially the starting composition for x = 0.1 and 0.2. For x = 0.5, the phases present were brannerite ($U_{0.8}Ca_{0.2}Ti_2O_6$), pyrochlore-structured $Ca_{1.2}U_{0.8}Ti_{2.1}O_7$ and rutile. These results indicated limiting Ca solubilities of ~ 0.2 and 0.3 formula units in argon- and air-fired materials respectively.

To examine the above mentioned idea that the U valences in the doped samples were > +4, X-ray absorption spectroscopy data were obtained (see Figure 1) for two Ca-doped

($x = 0.2$) brannerites prepared in argon and air, as well as the tetravalent and hexavalent U standards, UTi_2O_6 and CaUO_4 respectively.

Within the experimental accuracy of ~ 0.2 eV, the position of the U L_{III} -edge from the Ca-substituted brannerite annealed in argon was identical to that from undoped brannerite, in which the U is tetravalent. However, the spectrum also displayed slight asymmetric broadening on the high-energy side of the edge along with a reduced normalised intensity, suggesting that a small proportion of higher U valence states is present. This asymmetric broadening has been marked in Figure 1 with an arrow and is very pronounced in hexavalent U compounds, such as CaUO_4 , along with a shift in the position of the edge to higher energy. Materials that contain only a small proportion of U valence states $> +4$ typically display asymmetric broadening and a reduction in the normalised intensity of the edge prior to a discernible shift in the position of the edge to higher energy. The position of the U L_{III} -edge from the air fired Ca-substituted brannerite was slightly higher than in the argon anneal, and the asymmetry more pronounced, both of which indicate that the U was slightly more oxidised in the air fired Ca-substituted brannerite than in the parallel sample prepared in argon. Had the U valences been found to be +4, the indication would have been that oxygen vacancies were present.

To obtain further U valence state information, DRS measurements were made on stoichiometric UTi_2O_6 , and the two $x = 0.2$ samples fired in air and argon. In U-doped zircon for example, U^{4+} gives electronic absorption peaks through the range of 400-2000 nm, but U^{5+} yields peaks only in the 1000-1500 nm range[9]. No absorption peaks were observed by DRS in UTi_2O_6 [6], but the argon- and air-fired Ca-doped samples both

yielded a peak at 1448 nm, with possibly a weak extra peak near 1670 nm-see Fig. 2 below and [6]. In UTi_2O_6 brannerite, the absence of observable absorption peaks was previously interpreted [6] as showing that there are no isolated U^{4+} ions, but a more likely possibility is that because the U^{4+} site has a centre of inversion ($2/m$ point symmetry [3,4]), electric dipole transitions are forbidden, although weak vibronic absorptions might be expected. The weak absorption peaks at 1448 and possibly 1670 nm in the Ca-doped samples are attributed to U^{5+} ions; it would seem very possible that the substitution of U^{5+} in the U site with local charge compensation by Ca (also on U sites) causes a loss of inversion symmetry, allowing relatively sharp and intense zero-phonon electric dipole transitions. Green fluorescence characteristic of U^{6+} was not observed in either the air- or argon-fired samples upon ultraviolet irradiation.

The limiting solubility of Ca with all the U existing as U^{5+} would correspond to $\text{U}_{0.67}\text{Ca}_{0.33}\text{Ti}_2\text{O}_6$, a composition close to the observed limiting Ca solubility in air-fired material. In brannerites fired in argon, the occurrence of U solely as U^{4+} in pure brannerite and mixtures of U^{4+} and higher valence states in the Ca-doped materials shows the important role crystal-chemical effects play in determining valences of actinide ions.

Gd additions: $\text{U}_{1-x}\text{Gd}_x\text{Ti}_2\text{O}_{6-z}$. When fired in air, the $x = 0.1$ and 0.2 brannerites contained ~ 0.32 f.u of Gd; other phases were U_3O_8 and rutile. The $x = 0.5$ sample fired in air was almost single phase, corresponding to the limiting value expected if all the U is present as U^{5+} . A sample prepared with $x = 0.8$ resulted in brannerite of composition $\text{U}_{0.5}\text{Gd}_{0.5}\text{Ti}_2\text{O}_6$ with pyrochlore-structured $\text{Gd}_{1.73}\text{U}_{0.05}\text{Ti}_{2.16}\text{O}_7$ and rutile present as the other phases.

Single-phase brannerites of the starting compositions were obtained for $x = 0.1$ and 0.2 after firing in argon, but for $x = 0.5$, only $\sim 60\%$ of the sample consisted of brannerite ($\text{U}_{0.55}\text{Gd}_{0.45}\text{Ti}_2\text{O}_6$) with the rest being pyrochlore-structured $\text{Gd}_{1.69}\text{U}_{0.08}\text{Ti}_{2.15}\text{O}_7$ and rutile. DRS measurements on the $x = 0.2$ sample fired in argon yielded similar results to those obtained for the Ca -doped samples (see Fig. 2) and no ultraviolet-induced fluorescence characteristic of U^{6+} was observed. Similar but less detailed results were obtained with Y and La doping.

(3) Ca and Gd solubility in ThTi_2O_6

Notwithstanding the above arguments favouring U^{5+} formation to explain why Ca/Gd additions were able to stabilise brannerite formation in air, it was of interest to study the solubilities of Ca and Gd in thorutite (ThTi_2O_6 , isostructural with brannerite) in which actinide valence states $> 4+$ cannot be present. The solubility of Ca was found to be very small (< 0.01 f.u.); extra phases were rutile and perovskite with the reaction in the first instance being: $\text{Th}_{(1-x)}\text{Ca}_x\text{Ti}_2\text{O}_6 \rightarrow (1-x)\text{ThTi}_2\text{O}_6 + x \text{CaTiO}_3 + x \text{TiO}_2$. However some solubility of Th in the perovskite phase was apparent ($\text{Ca}_{0.78}\text{Th}_{0.11}\square_{0.11}\text{TiO}_3$), where \square represents a Ca vacancy required to effect overall charge neutrality (see also [8]). The solubility of Gd in the brannerite structure was measured as 0.1 f.u., with the formation of additional Th-doped pyrochlore. One might expect fairly similar results to be obtained with La, and Mitchell and Chakhmouradian[10] found the solubility of La in ThTi_2O_6 to be < 2.4 wt% (0.06 f.u.). The reaction for the Gd-doped sample can be written in the first instance as:

$\text{Th}_{(1-x)}\text{Gd}_x\text{Ti}_2\text{O}_6 \rightarrow (1-x) \text{ThTi}_2\text{O}_6 + (x/2) \text{Gd}_2\text{Ti}_2\text{O}_7 + x \text{TiO}_2$. However as mentioned above, there was restricted solubility of Gd in the Th-brannerite, and Th solubility in the pyrochlore, with the composition of the pyrochlore in the $x = 0.2$ material being given by approximately $\text{Gd}_{1.5}\text{Th}_{0.3}\text{Ti}_{2.1}\text{O}_7$.

Thus as expected on the basis that there are additional charge compensation mechanisms available in U-brannerite via U valence states $> +4$, relative to Th-brannerite, the solubilities of Gd and Ca in the Th-brannerite are much smaller than those in U-brannerite. The slight solubility of Gd in ThTi_2O_6 may involve a degree of oxygen deficiency.

As a final point on the question of stabilising brannerite via oxygen vacancies, it was found that UTi_2O_6 was not stable on heating for 16 h at 1300°C in 3.5% H_2/N_2 , with decomposition to UO_2 plus unidentified (presumably reduced Ti) oxides.

(4) Natural brannerite

DRS measurements on an argon- annealed natural brannerite sample [6] from Spain showed a peak at 1448 nm, as found for the synthetic Ca- and Gd-doped samples described above, together with weak peaks at 1670, 2070, and 2220 nm. This sample contained nearly 0.3 f.u. of Ca plus 0.03 f.u. of Y + rare earths substituting for U [11]. For the unannealed sample which was X-ray amorphous, the corresponding main peak was broader and more intense, as well as occurring at a lower energy, corresponding to 1520 nm (see Fig. 2). There were also other weaker peaks at 1690, 1950, and 2200 nm. The shifts in the spectral peaks reflect the altered crystal field of U^{5+} ions upon amorphisation. The absence of peaks attributable to U^{4+} suggests that these sites

essentially retain inversion symmetry even upon amorphization of the structure, although broadening would also inhibit their visualization.

X-ray absorption measurements were also undertaken on this sample (see Fig. 3). The position and shape of the U L_{III} -edge from the metamict natural brannerite sample to a first approximation coincided with that from $CaUO_4$, indicating that the majority of the U was hexavalent. Significantly, recrystallizing the metamict brannerite by annealing in argon at 1300°C also reduced the average U valence to just over 4+, as evidenced by the L_{III} edge shift.

(5) Other ions in brannerite

Other ions contained in natural brannerites include Nb and Fe[1,2,12]. In the ceramics for Pu disposition [4,5], Hf was of interest as neutron absorber and Ce as a simulant of Pu. Pu was of interest in its own right for the radioactive waste immobilisation application. The solid solubilities of these were explored in synthetic materials by the same methods described above, with the materials produced as before and fired at 1400°C. The solid solubility results, in formula units, are shown in Table I.

Yields of brannerite-structured PuTi_2O_6 were near-zero for firing temperatures below 1450°C, and ~ 75% on heating for 16 h at 1525°C, a temperature which was deduced to be close to the melting point of the PuTi_2O_6 . Although it is evidently difficult to synthesize end-member PuTi_2O_6 , there is no difficulty in synthesizing brannerite in which Pu is incorporated in dilute solid solution with the neutron absorbers, Hf and Gd, as used in pyrochlore-rich ceramics [4,5].

IV. Conclusions and Final Remarks

While brannerite, UTi_2O_6 , can only be formed under low oxygen pressures (approximately 10^{-5} atm.), the substitution of Ca and rare earths for U increase the stability of brannerite in atmospheres of increased oxygen activity. Ca and rare earths can be extensively substituted for U in both air-fired brannerite, and charge compensate for U valence states $> +4$, as shown by X-ray absorption spectroscopy. Significantly, almost as much Ca and rare earths can be substituted for U in neutral atmospheres, such as argon, as can be in air, illustrating the important dependence of actinide valence on crystal

chemistry as well as oxygen activity in the firing atmosphere. The absence of measurable solid solubility of Ca in brannerite-structured ThTi_2O_6 is taken as further evidence that Ca solubility in UTi_2O_6 takes place through the formation of U valence states $> +4$. Diffuse reflectance spectroscopy showed evidence of U^{5+} via an electronic absorption band near 1450 nm in the Ca/rare earth-doped samples fired in both air and argon, as well as in a natural sample. Other substitutions, such as Hf and Pu for U, $\text{Gd}^{3+} + \text{Nb}^{5+}$ for $\text{U}^{4+} + \text{Ti}^{4+}$, and Fe for Ti, are also possible.

Acknowledgments:

This work was supported in part by the Environmental Management Science Program of the US Department of Energy and partly by the Lawrence Livermore National Laboratory. The XANES work was conducted at the Stanford Synchrotron Research Laboratory (SSRL) which is operated by the US Department of Energy, Office of Basic Energy Sciences. We wish to thank S. Thomson and V. Luca for help with the diffuse reflectance spectroscopy, A. Brownscombe and M. Stewart for preparing the Pu-doped samples, and B. Ebbinghaus and D. Strachan for helpful discussions.

References

1. J.T. Szymanski and J.D. Scott, "A crystal-structure refinement of synthetic brannerite, UTi_2O_6 , and its bearing on rate of alkaline-carbonate leaching of brannerite in ore", *Canad. Mineral.*, 20, 271-9 (1982).
2. J.E. Patchett and E.W. Nuffield, "Studies of radioactive compounds. X. The synthesis and crystallography of brannerite". *Canad. Mineral.*, 6, 483-90 (1960).
3. A.E. Ringwood, S.E. Kesson, N.G. Ware, W. Hibberson and A. Major, "Immobilisation of High Level Nuclear Wastes in SYNROC", *Nature (London)*, 278, 219-23 (1979).
4. B.B. Ebbinghaus, R.A. VanKonynenburg, F.J. Ryerson, E.R. Vance, M.W.A. Stewart, A. Jostsons, J.S. Allender, T. Rankin and J. Congdon, "Ceramic Formulation for the Immobilization of Plutonium", *Waste Management '98* (CD-ROM; sess65/65-04), Tucson, AZ, USA, March 5, 1998.
5. E.R. Vance, M.W.A. Stewart, R.A. Day, K.P. Hart, M.J. Hambley and A. Brownscombe, "Pyrochlore-rich Titanate ceramics for Incorporation of Plutonium, Uranium and Process Chemicals", ANSTO report (1997).
6. E. R. Vance, J. N. Watson, M. L. Carter, R. A Day, G. R. Lumpkin, K. P. Hart, Y. Zhang, P. J. McGlinn, M. W. A. Stewart and D. J. Cassidy, "Crystal chemistry, radiation effects and aqueous leaching of brannerite, UTi_2O_6 ", *Proceedings of Nuclear Waste Management Symposium at American Ceramic Society Annual Meeting*, Indianapolis, April 28, 1999, in press.

7. A.E. Ringwood, S.E. Kesson, K.D. Reeve, D.M. Levins and E.J. Ramm, "Synroc", pp. 223-334 in *Radioactive Waste Forms for the Future*, Edited by W. Lutze and R.C. Ewing, Elsevier, (1988).
8. E.R. Vance, R.A. Day, Z. Zhang, B.D. Begg, C.J. Ball, M.G. Blackford, "Charge Compensation in Gd-doped CaTiO_3 ", *J. Solid State Chem.*, 124, 77-82 (1996).
9. E.R. Vance and D.J. Mackey, "Optical studies of U^{4+} and U^{5+} in zircon, hafnon and thorite", *Phys. Rev. B*, 18, 185-90 (1978).
10. R. H. Mitchell and A. R. Chakhmouradian, "Solid solubility in the system $\text{NaLREETi}_2\text{O}_6\text{-ThTi}_2\text{O}_6$ (LREE, light rare earth elements): experimental and analytical data", *Phys. Chem. Miner.* 26, 396-405 (1999).
11. G. R. Lumpkin, S. H. F. Leung, and M. Colella, "Composition, Geochemical Alteration, and Alpha-Decay Damage Effects of Natural Brannerite", in *Scientific Basis for Nuclear Waste Management XXIII*, Ed. D. Shoesmith, Materials Research Society, Pittsburgh, PA, USA, (2000), in press.
12. A. Pabst, Brannerite from California, *Amer. Mineral.*, 39, 109-17 (1954).

List of Tables

Table I. Solid solution limits for a variety of substitutions in brannerite prepared at 1400°C in either air or argon.

Substitution	1400°C Air	1400°C Argon
$(\text{U}_{1-x}\text{Hf}_x)\text{Ti}_2\text{O}_6$	0.24 [*]	0.24
$(\text{U}_{1-x}\text{Fe}_x)\text{Ti}_2\text{O}_6$	> 0.4	
$(\text{U}_{1-x}\text{Gd}_x)(\text{Ti}_{2-x}\text{Nb}_x)\text{O}_6$		0.7
$(\text{U}_{1-x}\text{Pu}_x)\text{Ti}_2\text{O}_6$	1	

^{*} determined with the Ce analogue of brannerite, CeTi_2O_6

List of Figures.

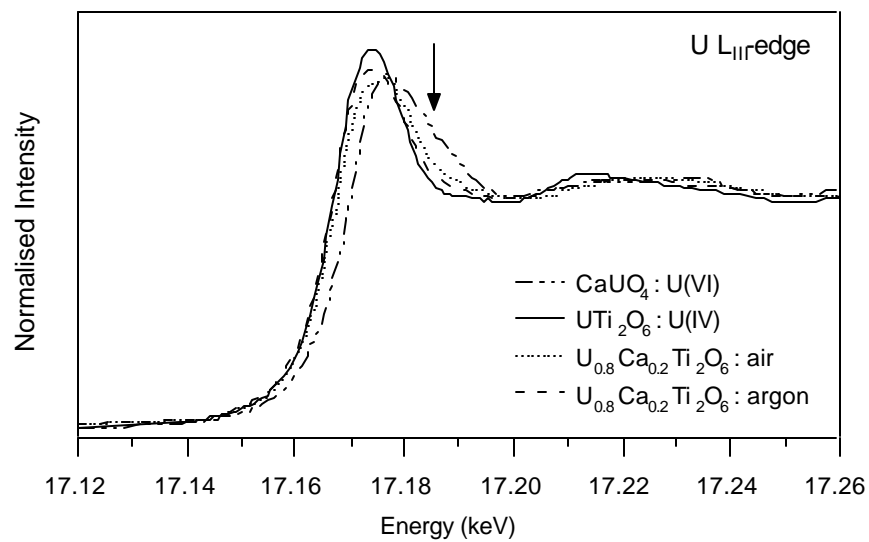


Figure 1. U L_{III}-edge XANES spectra from two Ca-substituted brannerites, U_{0.8}Ca_{0.2}Ti₂O₆ annealed in air and argon along with the tetra- and hexavalent U standards, UTi₂O₆ and CaUO₄ respectively.

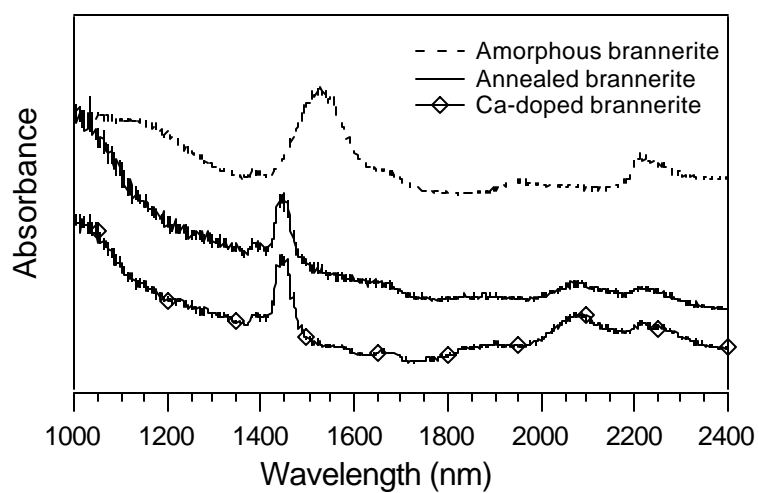


Fig. 2. Absorbance vs. wavelength for diffuse reflectance spectra of natural and synthetic brannerite. Spectra from an X-ray amorphous natural brannerite before and after annealing in argon at 1300°C are shown, along with that from a Ca-doped synthetic brannerite [6].

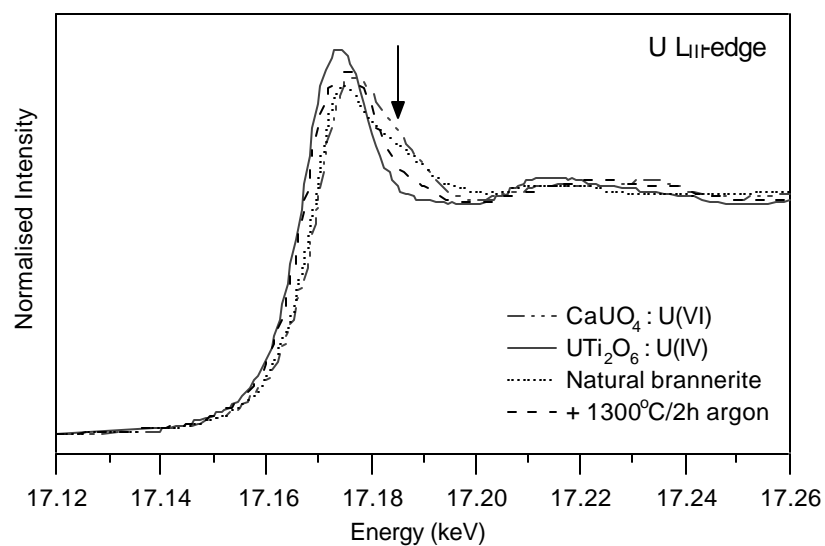


Figure 3. U L_{III}-edge XANES spectra from amorphous natural brannerite, before and after annealing in argon at 1300°C for 2 hours, along with the tetra- and hexavalent U standards, UTi_2O_6 and CaUO_4 respectively.